

Dark energy in rich clusters of galaxies

G.S.Bisnovatyi-Kogan *

Space Research Institute, Profsoyuznaya str. 84/32, Moscow 117997, Russia, and National Research Nuclear University "MEPHI", Kashirskoye Shosse, 31, Moscow 115409, Russia
E-mail: gkogan@iki.rssi.ru

Dark energy limits a radius of big clusters of galaxies, and may accelerate hot gas outflowing from the clusters as a wind. Collision of accelerated winds, in presence of a magnetic field, produce a situation favorable for acceleration of EHECR.

*Frontier Research in Astrophysics Workshop (FRAPWS2014)
26-31 May 2014
Palermo, Italy*

*Speaker.

1. Introduction

The value of Λ established by observations of SN Ia at redshift $z \leq 1$ (Riess et al., 1998; Perlmutter et al., 1999), and in the spectrum of fluctuations of the cosmic microwave background radiation (CMB), see e.g. Spergel et al. (2003), Tegmark et al. (2004). It was shown by Chernin (2001, 2008) that outer parts of galaxy clusters (GC) may be under strong influence of the dark energy (DE). DE is related to all kinds of the energy, having equation of state $P = -\beta\varepsilon$, with β close to unity, but may be not exactly equal to it. The Einstein cosmological constant Λ is now among the possible candidates for DE. The hot gas in the galactic clusters may flow outside due to high thermal pressure, and in the outer parts of the cluster the presence of a dark energy (DE) facilitates the outflow. A solution is presented of hydrodynamic equations for the winds from galactic clusters in presence of DE. It is a generalized solution for the outflows from the gravitating body, obtained for solar and stellar winds by Stanyukovich (1955) and Parker (1963), to the presence of DE. It implies significant changes in the structure of solutions describing galactic winds, what had been investigated in the paper of Bisnovaty-Kogan and Merafina (2013).

2. Accelerating expanding universe

Foundation of the view about expanding universe had been established in theoretical works of A. Friedmann and G. Lemaitre, and was confirmed by astronomical observations of E. Hubble. The equation for the scale factor $a(t)$ in the uniform isotropic universe is described by the equation, derived by A. Friedmann (see e.g. Bisnovaty-Kogan, 2011):

$$\frac{\dot{a}^2}{a^2} + \frac{kc^2}{a^2} = \frac{8\pi G}{3c^2}\varepsilon + \frac{\Lambda}{3}c^2. \quad (2.1)$$

This equation is combined with the relation of adiabatic expansion as $\frac{d\varepsilon}{\varepsilon+P} = -\frac{dV}{V} = -3\frac{da}{a}$, V is a volume. Let us consider a flat infinite universe with $k = 0$, and ultrarelativistic equation of state $P = \varepsilon/3$ The equations (2.1) is reduced to

$$\frac{\dot{a}^2}{a^2} = \frac{8\pi G}{3c^2}\varepsilon + \frac{\Lambda}{3}c^2, \quad \varepsilon = \rho c^2 = \rho_* c^2 \frac{a_*^4}{a^4}, \quad (2.2)$$

which has a solution in the form

$$\frac{dx}{dt} = 2\sqrt{\frac{8\pi G\rho_*}{3}a_*^4 + \frac{\Lambda}{3}c^2x^2}, \quad x = a^2, \quad a^2 = a_*^2\sqrt{\frac{8\pi G\rho_*}{\Lambda c^2}} \sinh\left(2\sqrt{\frac{\Lambda}{3}}ct\right). \quad (2.3)$$

At the beginning of expansion, at small t we have a solution

$$a^2 = a_*^2 t \sqrt{\frac{32\pi}{3}G\rho_*}, \quad \rho = \frac{3}{32\pi G t^2}, \quad (2.4)$$

and for large t there is an exponential expansion at non-zero cosmological constant:

$$a^2 = \frac{a_*^2}{2} \sqrt{\frac{8\pi G\rho_*}{\Lambda c^4}} \exp\left(2\sqrt{\frac{\Lambda}{3}}ct\right), \quad \rho = \frac{\Lambda c^4}{2\pi G} \exp\left(-4\sqrt{\frac{\Lambda}{3}}ct\right). \quad (2.5)$$

The model of the hot universe was suggested by G. Gamow, and was confirmed by A. Penzias and R. Wilson, discovering a cosmic microwave background (CMB). To overcome some problems existing in pure Friedmann universe, it was suggested that the very initial stages of the universe expansion follow exponential growth of the scaling factor with time (de Sitter expansion), what was anticipated in 1965 by Gliner (1965). The de Sitter stage in the early universe is created not by existence of the cosmological constant, like in the original de Sitter work, but by a physical substance, such like a scalar field, or an "excited vacuum", which mimic the cosmological constant, having the vacuum equation of state $P = -\epsilon$. The accelerated expansion is accompanied by a transformation of the energy of the scalar field into the energy of the ordinary matter, so that the de Sitter state is transformed into the Friedmann expansion. The stage before installing the Friedmann expansion was named as inflation. Non-zero Lambda term, much smaller than during inflation, was discovered by the observations of distant SN Ia, and CMB fluctuations, so presently we live during the transition stage from Friedmann expansion to exponential expansion stage.

For discovery of the expansion law of the present universe we need independent measurements of the velocity, and distance to very remote objects, such like galaxies, quasars, galaxy clusters. Observations of Supernovae Ia events, which are thermonuclear explosions in the degenerate CO core, are used for these purposes, due to possibility to find its total luminosity by measurements of its light curve (some type of a standard candle). The most well known examples of SN Ia remnants in our galaxy are the remnants of SN 1572, which explosion was observed by Tycho Brahe, and of SN 1604, observed by J. Kepler.

Two sky surveys for search of distance SN Ia in distant galaxies had been performed by two groups of researchers. The results of the first group, were published in two papers by Riess et al. (1998), and Schmidt et al.(1998).

"Observational Evidence from Supernovae for an Accelerating Universe and a Cosmological Constant" by Riess A.G.+ 19 authors, where 10 SNIa, with $0.16 \leq z \leq 0.62$ were observed, and "The High-Z Supernova Search: Measuring Cosmic Deceleration and Global Curvature of the Universe Using Type Ia Supernovae" by Schmidt B.P.+ 23 authors, where 30 SNIa, with $0.35 \leq z \leq 0.9$ were observed had shown the existence of a non-zero cosmological constant, with parameters $\Omega_M = 0.4^{+0.5}_{-0.4}$, $\Omega_\Lambda = 0.6^{+0.4}_{-0.5}$. It was claimed that unless supernovae are much different at high redshifts, the imperfection of SNe Ia as distance indicators will have a negligible impact on using SNe Ia as cosmological probes.

In the first paper, published by a second group, no cosmological constant was found. Here (Perlmutter et al., 1997)+ 23 authors from "The Supernova Cosmology Project", in the paper titled "Measurements of the Cosmological Parameters Ω and Λ from the First Seven Supernovae at $z \geq 0.35$ " it was claimed that "for a spatially flat universe ($\Omega_M + \Omega_\Lambda = 1$), we find $\Omega_M = 0.94^{+0.34}_{-0.28}$ or, equivalently, a measurement of the cosmological constant, $\Omega_\Lambda = 0.06^{+0.28}_{-0.34}$ ". After appearance of papers of Riess et al.(1998), and Schmidt et al. (1998) the second paper was published, where (Perlmutter et al, 1999) with 32 authors from "The Supernova Cosmology Project", in the paper "Measurements of Omega and Lambda from observations of 42 High-Redshift Supernovae", where SH Ia redshifts were between 0.18 and 0.83, claimed the existence of a nonzero cosmological constant in the flat universe. In the Fig,2 from Perlmutter et al, (1999) this result follows from a comparison of the observational data with predictions of theoretical models.

Measurements of Cosmic Microwave Background fluctuations, made from satellites Relikt,

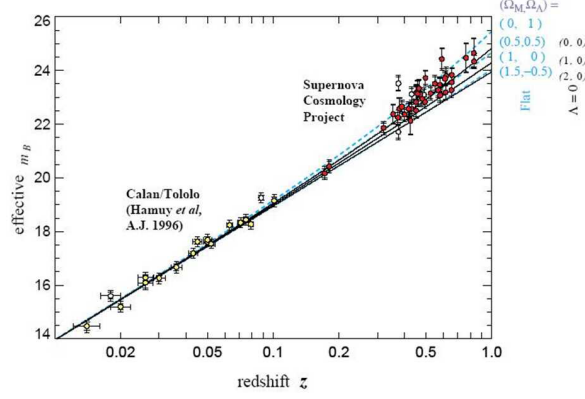


Figure 1: Hubble diagram for 42 high-redshift Type Ia supernovae from the Supernova Cosmology Project, and 18 low-redshift Type Ia supernovae from the Calán/Tololo Supernova Survey, after correcting both sets for the SN Ia lightcurve width-luminosity relation. The inner error bars show the uncertainty due to measurement errors, while the outer error bars show the total uncertainty when the intrinsic luminosity dispersion, 0.17 mag, of lightcurve-width-corrected Type Ia supernovae is added in quadrature. The unfilled circles indicate supernovae not included in Fit C. The horizontal error bars represent the assigned peculiar velocity uncertainty of 300 km s^{-1} . The solid curves are the theoretical $m_B^{\text{effective}}(z)$ for a range of cosmological models with zero cosmological constant: $(\Omega_M, \Omega_\Lambda) = (0, 0)$ on top, $(1, 0)$ in middle and $(2, 0)$ on bottom. The dashed curves are for a range of flat cosmological models: $(\Omega_M, \Omega_\Lambda) = (0, 1)$ on top, $(0.5, 0.5)$ second from top, $(1, 0)$ third from top, and $(1.5, -0.5)$ on bottom.

COBE, WMAP (2001), Planck (2006), and balloons: Boomegang, Maxima, CBI, ACBAR, etc, had established a model of a flat hot universe at $\Omega_{\text{tot}} = 1$, and distribution between different types of matter as: dark energy (Λ term) $\Omega_\Lambda \approx 0.7$, dark matter (nonbarionic dark matter) $\Omega_{\text{DM}} \approx 0.26$, baryonic $\Omega_B = 0.04$.

Equilibrium Planck radiation with temperature about 3 K was left as a result of expansion of the hot universe, together with relict neutrino, and gravitons. Matter had separated from the radiation at redshift $z \sim 1000$. Radiation preserves non-uniformities of that period. Study of CMB fluctuations permitted to evaluate the global parameters of the universe: Ω and its ingradients, H (Hubble constant), determining the rate of the universe expansion around us: $V = Hr$, $H \sim 70 \text{ km/s/Mpc}$.

First results of Planck observation of CMB fluctuations have shown some differences from earlier results for most cosmological parameters. The example of these correction to the Hubble constant is shown in Fig.3 from Planck Collaboration (2013). Another corrections obtained from Planck observations are listed in the Table.1 from the same paper.

Planck results gave new estimation of Ω_Λ , H_0 , and put restrictions to the neutrino rest mass. and primordial helium fraction Y_0 . The Hubble constant in different measurements is presented in Tabl.1 from Planck Collaboration (2013). Recently it was found by Spergel et al.(2013), that the $217 \text{ GHz} \times 217 \text{ GHz}$ detector set spectrum used in the Planck analysis, is responsible for some of discrepancies with WMAP data. Another data analysis was done, which uses 47% of the sky and makes use of both 353 and 545 GHz data for foreground cleaning. It was found that the Λ CDM cosmological parameters $\Omega_c h^2 = 0.1169 \pm 0.0025$, $n_s = 0.9671 \pm 0.0069$, $H_0 = 68.0 \pm 1.1 \text{ km s}^{-1} \text{ Mpc}^{-1}$, $\Omega_b h^2 = 0.02197 \pm 0.00027$, $\ln 10^{10} A_s = 3.080 \pm 0.025$, and $\tau = 0.089 \pm 0.013$.

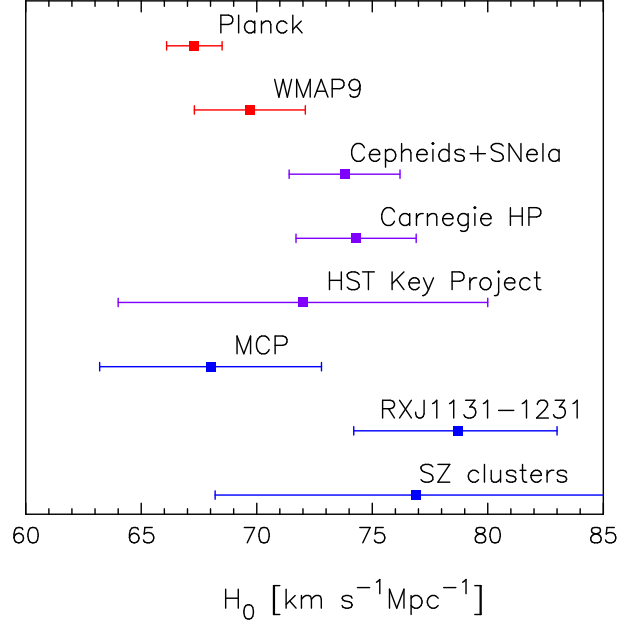


Figure 2: Comparison of H_0 measurements, with estimates of $\pm 1 \sigma$ errors, from a number of techniques. These are compared with the spatially-flat LCDM model constraints from Planck and WMAP.

Parameter	Planck+WP	Planck+WP+BAO	WMAP-9
$\Omega_b h^2$	0.02206 ± 0.00028	0.02220 ± 0.00025	0.02309 ± 0.00130
$\Omega_c h^2$	0.1174 ± 0.0030	0.1161 ± 0.0028	0.1148 ± 0.0048
τ	0.095 ± 0.014	0.097 ± 0.014	0.089 ± 0.014
H_0	65.2 ± 1.8	66.7 ± 1.1	74 ± 11
n_s	0.974 ± 0.012	0.975 ± 0.012	0.973 ± 0.014
$\log(10^{10} A_s)$	3.106 ± 0.029	3.100 ± 0.029	3.090 ± 0.039
α/α_0	0.9936 ± 0.0043	0.9989 ± 0.0037	1.008 ± 0.020

Table 1: Constraints on the cosmological parameters of the base LCDM model with the addition of a varying fine-structure constant. $\pm 1 \sigma$ errors are quoted.

While in broad agreement with the results reported by the Planck team, these revised parameters imply a universe with a lower matter density of $\Omega_m = 0.302 \pm 0.015$, and parameter values generally more consistent with pre-Planck CMB analyses and astronomical observations.

All perturbations are correlated, so to the moment of recombination amplitudes of harmonics oscillate, showing Doppler peaks which are called also as Sakharov oscillations (Sakharov, 1965). The results of 7 years operation of WMAP for power spectrum of CMB temperature fluctuations, from Larson et al (2011), and same value measured by Planck from Planck Collaboration (2013), are presented in fig.4.

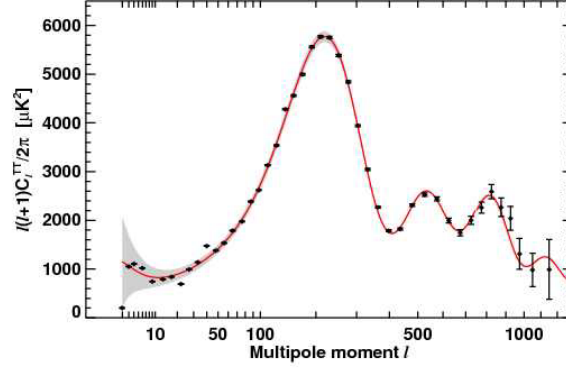


Figure 3: The 7-year temperature (TT) power spectrum from WMAP. The third acoustic peak and the onset of the Silk damping tail are well measured. The curve is the Λ CDM model best fit: $\Omega_b h^2 = 0.02270$, $\Omega_c h^2 = 0.1107$, $\Omega_\Lambda = 0.738$. From Larson et al.(2011).

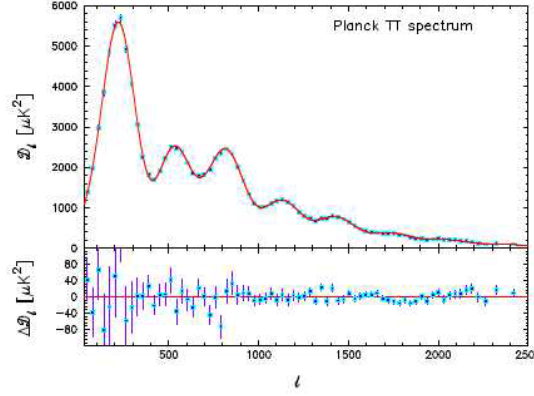


Figure 4: Planck temperature (TT) power spectrum. The points in the upper panel show the maximum-likelihood estimates of the primary CMB. The red line shows the best-fit base Λ CMD spectrum. The lower panel shows the residuals with respect to the theoretical model. The error bars are indicated. From Planck Collaboration (2013).

3. DE influence on the structure of galactic clusters

In papers of Chernin (2001),(2008) the question was raised about a possible influence of the existence of the cosmological constant on the properties of the Hubble flow in the local galaxy cluster in close vicinity of our Galaxy. Basing on the observations of Karachentsev et al. (2006), he concluded that the presence of the the dark energy (DE) is responsible for the formation of this Hubble flow.

The importance of the DE for the structure of the galaxy cluster depends on the level of the influence of DE on the dynamic properties. In particular, it is necessary to check,when the cluster may exist in the equilibrium state, at present values of DE density, and the densities of matter, consisting of the baryonic, and dark matter (BM and DM). This problem was investigated in papers of Bisnovatyi-Kogan and Chernin (2012), and Chernin et al. (2013), where the structure of galaxy clusters halo in Virgo and Coma were analysed. It was obtained that the key physical parameters

of the dark matter halos in clusters are determined by dark energy:

(1) the halo cut-off radius is practically, if not exactly, equal to the zero-gravity radius at which the dark matter gravity is balanced by the dark energy antigravity;

(2) the halo averaged density is close to two densities of dark energy.

Dark energy is a relativistic fluid and its description is based on General Relativity. Nevertheless it may be treated in terms of the Newtonian mechanics, if the force field it produces is weak in the ordinary accepted sense. The Newtonian treatment borrows from General Relativity the major result: the effective gravitating density of a uniform medium is given by the sum $\rho_{eff} = \rho + 3p$. With its equation of state $p_\Lambda = -\rho_\Lambda$, the dark energy has a negative effective gravitating density:

$$\rho_{\Lambda eff} = \rho_\Lambda + 3p_\Lambda = -2\rho_\Lambda < 0, \quad F(r) = F_N(r) + F_E(r) = -G\frac{M}{r^2} + \frac{8\pi G}{3}\rho_\Lambda r. \quad (3.1)$$

which means that dark energy produces antigravity. Eq. (3.1) shows that the net force $F(R)$ is zero at the distance

$$R = R_{ZG} = \left[\frac{M_M}{\frac{8\pi}{3}\rho_{DE}} \right]^{1/3} = 11 \frac{M_M}{10^{15}M_\odot} \text{ Mpc}. \quad (3.2)$$

Here the observed value of the dark energy density $\rho_{DE} = 0.7 \times 10^{-29} \text{ g/cm}^3$ is used. The critical physical parameter R_{ZG} is the zero-gravity radius (Chernin 2001). Gravity dominates at distances $R < R_{ZG}$, while antigravity is stronger than gravity at $R > R_{ZG}$.

If the radius of a system with matter mass M_M is equal to the maximal radius $R = R_{max}$, its mean matter density (see Bisnovatyi-Kogan & Chernin 2012) is $\langle \rho_M \rangle = \frac{M_M}{\frac{4\pi}{3}R_{ZG}^3} = 2\rho_{DE}$, where the mass of Virgo cluster was estimated as $\sim 6 \times 10^{14} M_\odot$, and its radius as $\sim 10 \text{ Mpc}$. The mass and radius of the Coma cluster at zero gravitation radius are estimated as (Chernin et al., 2013)

$$R_{max} = R_{ZG} = 20 \text{ Mpc}, \quad M(R_{ZG}) = 6.2 \times 10^{15} M_\odot, \quad (3.3)$$

If this is the case, the mean matter density of the system is equal to twice the dark energy density. This prediction (Merafina et al. 2012; Bisnovatyi-Kogan & Chernin 2012) does not depend on the density profile assumed for the cluster.

4. Newtonian approximation in description of galactic winds in presence of DE

The hot gas in the galactic clusters may flow outside due to high thermal pressure, and in the outer parts of the cluster the presence of a dark energy (DE) facilitates the outflow. In the Newtonian approximation, in presence of DE, we have the following hydrodynamic Euler equation for the spherically symmetric outflow in the gravitational field of matter and DE

$$\rho v \frac{dv}{dr} + \frac{dP}{dr} = -\rho \left(\frac{Gm_m}{r^2} - \frac{\Lambda c^2 r}{3} \right) = -\rho \left(\frac{Gm_m}{r^2} - \frac{8\pi G\rho_\Lambda r}{3} \right). \quad (4.1)$$

Here ρ and P are a matter density and pressure, respectively, m_m is the mass of the matter inside the radius r . We use here DE in the form of the Einstein cosmological constant Λ . Newtonian gravitational potentials produced by matter Φ_g , and Φ_Λ by DE, satisfy the Poisson equations

$$\Delta\Phi_\Lambda = -8\pi G\rho_\Lambda, \quad \Delta\Phi_g = 4\pi G\rho, \quad \rho_\Lambda = \frac{\Lambda c^2}{8\pi G}. \quad (4.2)$$

We consider, for simplicity, the outflow in the field of a constant mass (like in stellar wind) $m_m = M$. The Eq. (4.1) in this case is written as

$$\rho v \frac{dv}{dr} + \frac{dP}{dr} = -\rho \left(\frac{GM}{r^2} - \frac{\Lambda c^2 r}{3} \right) = -\rho \left(\frac{GM}{r^2} - \frac{8\pi G\rho_\Lambda r}{3} \right). \quad (4.3)$$

The Eq. (4.1) should be solved together with the continuity equation in the form $4\pi\rho v r^2 = \dot{M}$, where \dot{M} is the constant mass flux from the cluster. We consider polytropic equation of state, where pressure P , and sound speed c_s are defined as

$$P = K\rho^\gamma, \quad c_s^2 = \gamma \frac{P}{\rho}, \quad \rho = \left(\frac{c_s^2}{\gamma K} \right)^{\frac{1}{\gamma-1}}, \quad P = \left(\frac{c_s^2}{\gamma} \right)^{\frac{\gamma}{\gamma-1}} K^{-\frac{1}{\gamma-1}}. \quad (4.4)$$

Introduce nondimensional variables as

$$\tilde{v} = \frac{v}{v_*}, \quad \tilde{c}_s = \frac{c_s}{c_*}, \quad \tilde{r} = \frac{r}{r_*}, \quad r_* = \frac{GM}{c_*^2},$$

$$v_* = c_*, \quad \tilde{\rho} = \frac{\rho}{\rho_*}, \quad \rho_* = \left(\frac{c_*^2}{\gamma K} \right)^{\frac{1}{\gamma-1}}, \quad \tilde{P} = \frac{P}{P_*}, \quad P_* = \left(\frac{c_*^2}{\gamma} \right)^{\frac{\gamma}{\gamma-1}} K^{-\frac{1}{\gamma-1}}. \quad (4.5)$$

In non-dimensional variables the equation (4.3) is written as

$$\tilde{v} \frac{d\tilde{v}}{d\tilde{r}} + \frac{2}{\gamma-1} \tilde{c}_s \frac{d\tilde{c}_s}{d\tilde{r}} + \frac{1}{\tilde{r}^2} - \lambda \tilde{r} = 0, \quad \lambda = \frac{\Lambda c_*^2 r_*^2}{3c_*^2}. \quad (4.6)$$

The continuity equation in non-dimensional form is written as

$$\tilde{\rho} \tilde{v} \tilde{r}^2 = \dot{m}, \quad \tilde{c}_s^{\frac{2}{\gamma-1}} \tilde{v} \tilde{r}^2 = \dot{m}, \quad \dot{m} = \frac{\dot{M}}{M_*}, \quad \dot{M}_* = 4\pi\rho_* v_* r_*^2. \quad (4.7)$$

It follows from (4.4),(4.5),(4.7), that

$$\frac{d\tilde{\rho}}{\tilde{\rho}} = \frac{2}{\gamma-1} \frac{d\tilde{c}_s}{\tilde{c}_s}, \quad \frac{d\tilde{\rho}}{\tilde{\rho}} + \frac{d\tilde{v}}{\tilde{v}} + 2\frac{d\tilde{r}}{\tilde{r}} = 0. \quad (4.8)$$

Using (4.8) we may write the equation of motion (4.4) in the form

$$\frac{d\tilde{v}}{d\tilde{r}} = \frac{\tilde{v}}{\tilde{r}} \frac{2\tilde{c}_s^2 - \frac{1}{\tilde{r}} + \lambda \tilde{r}^2}{\tilde{v}^2 - \tilde{c}_s^2}. \quad (4.9)$$

The only physically relevant solutions are those which pass smoothly the sonic point $v = c_s$, being a singular point of the Eq. (17), with $\tilde{v} = \tilde{c}_s$, $2\tilde{c}_s^2 - \frac{1}{\tilde{r}} + \lambda \tilde{r}^2 = 0$ where $\tilde{r} = \tilde{r}_c$, $\tilde{v} = \tilde{v}_c$, $\tilde{c}_s = \tilde{c}_{sc}$. Choosing $c_* = c_{sc}$, we obtain in the critical point

$$\tilde{v}_c = \tilde{c}_{sc} = 1, \quad 2 - \frac{1}{\tilde{r}_c} + \lambda \tilde{r}_c^2 = 0. \quad (4.10)$$

With this choice of the scaling parameters, we have from (4.7) $\dot{m} = \tilde{r}_c^2$. The physical meaning of the parameter λ becomes clear after rewriting it, using (4.2),(4.5), in the form

$$\lambda = \frac{\Lambda c^2 r_*^2}{3c_*^2} = \rho_\Lambda \frac{8\pi}{3M} r_*^3 = \rho_\Lambda \frac{8\pi}{3M} \frac{r_c^3}{\tilde{r}_c^3} = \frac{2\rho_\Lambda}{\rho_M} \frac{1}{\tilde{r}_c^3}, \quad (4.11)$$

where $\rho_M = \frac{3M}{4\pi r_c^3}$ is a density of the matter after smearing the central mass uniformly inside the critical radius r_c . The value of λ is proportional to the ratio of the dark energy mass inside the critical radius $M_\Lambda = \frac{4\pi}{3} r_c^3 \rho_\Lambda$ to the mass M of the central body.

The relation (4.10) determines the dependence $\tilde{r}_c(\lambda)$ in the solution for the galactic wind and accretion, in presence of DE. In presence of DE the critical radius of the flow is situated closer to the gravitating center (in non-dimensional units) with increasing λ . The Eq.(4.6) for the polytropic flow has a Bernoulli integral as

$$\frac{\tilde{v}^2}{2} + \frac{\tilde{c}_s^2}{\gamma-1} - \frac{1}{\tilde{r}} - \frac{\lambda \tilde{r}^2}{2} = h, \quad \tilde{c}_s^2 = \left(\frac{\dot{m}}{\tilde{v} \tilde{r}^2} \right)^{\gamma-1} = \left(\frac{\tilde{r}_c^2}{\tilde{v} \tilde{r}^2} \right)^{\gamma-1}. \quad (4.12)$$

The dimensional Bernoulli integral $H = hc_{sc}^2$. The Bernoulli integral is determined through the parameters of the critical point, with account of (4.10), as

$$h = \frac{\gamma+1}{2(\gamma-1)} - \frac{1}{\tilde{r}_c} - \frac{\lambda \tilde{r}_c^2}{2} = \frac{5-3\gamma}{2(\gamma-1)} - \frac{3}{2} \left(\frac{1}{\tilde{r}_c} - 2 \right). \quad (4.13)$$

The dependence $h(\lambda)$ for different polytropic powers γ is given in Fig.1. Note that in presence of DE the outflow is possible also for negative values of the Bernoulli integral h , defined equally.

The stationary solution for the wind is determined by two integrals: constant mass flux \dot{M} , and energy (Bernoulli) integral H . In absence of DE we obtain the known relations $\tilde{r}_c = \frac{1}{2}$, $h = \frac{5-3\gamma}{2(\gamma-1)}$. In the outflow from the physically relevant quasi-stationary object the antigravity from DE should be less than the gravitational force on the outer boundary, which we define at $r = r_*$. Therefore the value of Λ is restricted by the relation (see e.g. Bisnovatyi-Kogan and Chernin, 2012)

$$2\rho_\Lambda = \frac{\Lambda c^2}{4\pi G} < \bar{\rho} = \frac{4\pi M}{3r_*^3} \quad (4.14)$$

In non-dimensional variables this restriction, with account of (4.5),(4.6) is written as

$$\lambda < \frac{16\pi^2}{9} = 17.55 = \lambda_{lim}. \quad (4.15)$$

It is reasonable to consider only the values of λ smaller than λ_{lim} . It follows from (4.10), that \tilde{r}_c is monotonically decreasing with increasing λ . For $\lambda = \lambda_{lim} = 17.55$ we obtain $\tilde{r}_c = \tilde{r}_{c,lim} \approx 0.29$. The effective gravitational potential $\tilde{\Phi}$ is formed by the gravity of the central body, and antigravity of DE

$$\tilde{\Phi} = -\frac{1}{\tilde{r}} - \frac{\lambda \tilde{r}^2}{2}.$$

To overcome the gravity of the central body, the value of h should exceed the maximum value of the gravitational potential, defined by the extremum of $\tilde{\Phi}$

$$h \geq \tilde{\Phi}_{max}(\tilde{r}_{max}) = -\frac{3}{2}\lambda^{1/3}, \quad \tilde{r}_{max} = \lambda^{-1/3}. \quad (4.16)$$

It follows from(26), (35), that always $\tilde{r}_{max} > \tilde{r}_c$. So, in presence of DE the outflow of the gas from the cluster to the infinity is possible even at the negative values of h . In absence of DE the non-negative value of h , and the outflow are possible only at $\gamma \leq \frac{5}{3}$.

5. Solutions of the galactic wind equation in presence of DE

The equation (4.9) has a sound critical point of the saddle type, and two physical (critical) solutions going through this critical point. One of this solutions describes a wind outflow, and has a positive \tilde{v} . Another solution corresponds to an accretion (inflow), and has a negative \tilde{v} (Stanyukovich, 1955; Parker, 1963). To obtain a physically relevant critical solution of (4.9), with \tilde{c}_s^2 from (4.5), we obtain expansion in the critical point with $\tilde{v}^2 = \tilde{c}_s^2 = 1$, in the form

$$\begin{aligned} \tilde{v} &= 1 + \alpha(\tilde{r} - \tilde{r}_c), \quad \alpha_1 = -\frac{2}{\tilde{r}_c} \frac{\gamma-1}{\gamma+1} + \frac{1}{\tilde{r}_c} \frac{2}{\gamma+1} \sqrt{2 + \frac{1}{4\tilde{r}_c} + \frac{\lambda\tilde{r}_c^2}{2} - \gamma \left(2 - \frac{1}{4\tilde{r}_c} - \frac{\lambda\tilde{r}_c^2}{2}\right)}, \\ \alpha_2 &= -\frac{2}{\tilde{r}_c} \frac{\gamma-1}{\gamma+1} - \frac{1}{\tilde{r}_c} \frac{2}{\gamma+1} \sqrt{2 + \frac{1}{4\tilde{r}_c} + \frac{\lambda\tilde{r}_c^2}{2} - \gamma \left(2 - \frac{1}{4\tilde{r}_c} - \frac{\lambda\tilde{r}_c^2}{2}\right)}. \end{aligned} \quad (5.1)$$

Here α_1 corresponds to the wind solution, and α_2 is related to the case of accretion where \tilde{v} define the absolute value. At $\lambda = 0$ we have a well known expansion with

$$\alpha_1 = \frac{4}{\gamma+1} \left[\sqrt{\frac{5-3\gamma}{2}} - (\gamma-1) \right], \quad \alpha_2 = -\frac{4}{\gamma+1} \left[\sqrt{\frac{5-3\gamma}{2}} + (\gamma-1) \right].$$

The numerical solution of (4.9) was obtained using predictor-corrector Runge-Kutta method of 4-th order, with a fixed relative precision, written in Fortran 77, see Press et al. (1992) The integration started from the critical point with $\tilde{v} = \tilde{c}_s = 1$, using the expansion (5.1), both inside and outside the critical point, for two types of the flow: the wind flow, corresponding to the coefficient α_1 in (5.1), and accretion flow, corresponding to α_2 in (5.1). The critical solutions of the equation (4.9), with account of (4.12), are presented in Figs.2,3 for different values of γ and λ . Both wind and accretion solutions are presented.

The wind and accretion solutions are plotted in the same figures 5,6, but the positive velocities correspond only to the wind solutions. The outflow solutions have increasing velocities in presence of DE with $\lambda > 1$, but at $\lambda = 0$ the behaviour at large radius \tilde{r} depends on the adiabatic power γ . The velocity is increasing in the wind solution at $\gamma = \frac{4}{3}$ (Fig.5). At $\gamma = \frac{5}{3}$ the wind solution has a decreasing outflow velocity with a constant Mach number Ma , see Fig.6.

The accretion solutions in Figs. 5,6 are represented by the absolute values of the inflow velocity $|\tilde{v}|$, and the inflow velocity during accretion has a negative sign. The inflow velocity inside the critical point at $\gamma = \frac{4}{3}$ at all λ converges to the same free fall velocity $\tilde{v} \rightarrow -\sqrt{\frac{2}{\tilde{r}}}$, according to the Bernoulli integral (4.12), with $\tilde{r} \ll 1$, in the supersonic flow with $\tilde{v} \gg \tilde{c}_s$. At $\gamma = \frac{5}{3}$ the inflow solution at $\tilde{r} \ll 1$ is approaching to the constant Mach number solution. The inflow solutions given in Fig.6 correspond to $Ma = 1$. The equation (4.9) is invariant to the transformation $\tilde{v} \rightarrow -\tilde{v}$, therefore the accretion solution was possible to obtain numerically for the absolute values of the velocity.

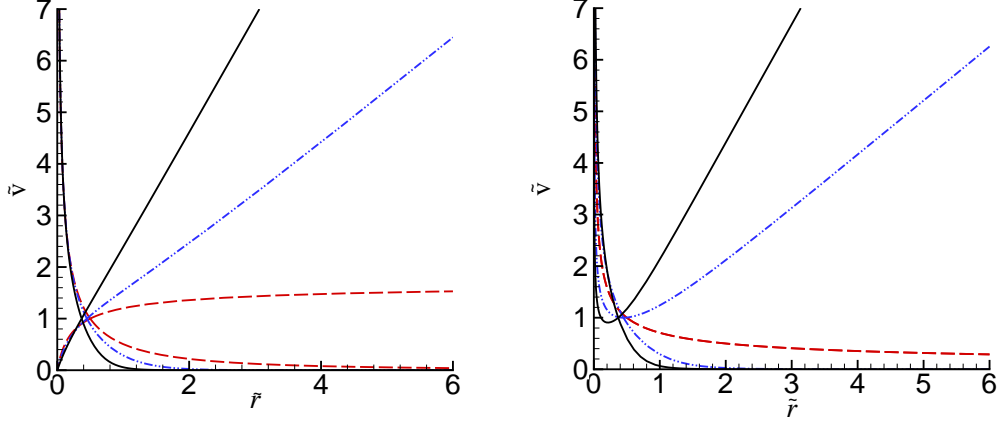


Figure 5: The integral curves of the wind and accretion solutions, for $\gamma = 4/3$ (left) and $\gamma = 5/3$ (right). Here $\lambda = 0$, $r_c = 0.5$ (dashed curve); $\lambda = 1.10$, $r_c = 0.45$ (dash-dot-dot curves); and $\lambda = 5.13$, $r_c = 0.37$ (full curves). For nonzero λ wind solutions correspond to curves with increasing velocity at large radius. The curves with decreasing velocities correspond to the accretion solution with negative v , so that its absolute values are presented. For $\gamma = 5/3$ at $\lambda = 0$ both wind and accretion solutions are presented by the same curve, which corresponds to the wind for positive v , and to the accretion for negative v .

The inflow solutions for the accretion starts at large radiuses by a slow motion to the gravitating center. The velocity increases in a subsonic regime, and after crossing the critical point the supersonic infall to the gravitating center starts. Note, that the accretion solutions have a physical sense only for small λ , when the region with a attractive gravitational force is sufficiently large. In the regions with repulsing force due to DE antigravity, the critical accretion solutions of the equation (4.9) formally exist, but they correspond to anomalous density distribution increasing with radius, what cannot be expected in reality.

6. Discussion

It is clear that the presence of DE tends to help the outflow of the hot gas from the gravitating object, as well as to the escape of rapidly moving galaxies (Chernin et al, 2013). Here we have obtained the solution for outflow in presence of DE, which generalize the well-known solution for the polytropic solar (stellar) wind. Presently the DE density exceed the density of the dark matter, and, even more, the density of the barionic matter. The clusters which outer radius is approaching the zero gravity radius, may not only loose galaxies, which join the process of Hubble expansion, but also may loose the hot gas from the outer parts of the cluster. Let us consider outer parts of the Coma cluster at radius $R_C = 15$ Mpc, with the mass inside $M_C = 5 \cdot 10^{15} M_\odot$, from Chernin et al. (2013). For the present value of $\rho_\Lambda = 0.71 \cdot 10^{-29}$ g/cm³, supposing that $R_C = r_*$ is the critical radius of the wind, we obtain from (4.2),(4.67), the nondimensional constant λ as

$$\lambda = \frac{\Lambda c^2 r_*^2}{3c_*^2} = \frac{8\pi \rho_\Lambda r_*^3}{3M} \approx 0.59, \quad c_* = \sqrt{\frac{GM_C}{R_C}} \approx 1200 \text{ km/c.} \quad (6.1)$$

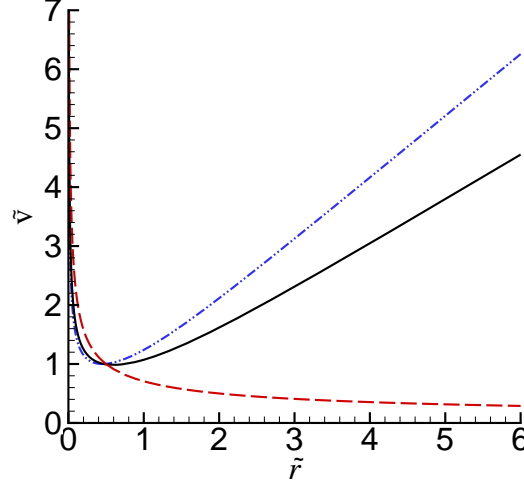


Figure 6: The integral curves for the wind solution, at $\gamma = 5/3$ and $\lambda = 0$, $r_c = 0.5$ (**dashed curve**); $\lambda = 1.10$, $r_c = 0.45$ (**dash-dot-dot curve**); and $\lambda = 0.58$, $r_c = 0.47$ (**full curve**)

It corresponds to the temperature about $T \approx 6 \cdot 10^7$ K, $kT \approx 5$ keV. Observations of the hot gas distribution in the Coma cluster (Watanabe et al., 1999) on ASCA satellite have shown a presence of hot region with $kT = 11 - 14$ keV, and more extended cool region with $kT = 5 \pm 1$ keV, what is in good accordance with our choice of parameters.

Wind solutions for $\lambda = 0; 0.58; 1.1$ are presented in Fig.7. The solution with $\lambda = 0.58$ is the closest to the description of the outflow from Coma cluster. The density of the gas in the vicinity of $r = r_c$ is very small, so the flow may be considered as adiabatic (polytropic) with the power $\gamma = 5/3$. Without DE such gas flow is inefficient, its velocity is decreasing $\sim 1/\sqrt{r}$. In presence of DE the wind velocity is increasing 2 times at the distance of $\sim 5r_c \sim 75$ Mpc from Coma.

After quitting the cluster the gas is moving with acceleration, acting as a snowplough for the intergalactic gas. The shell of matter, forming in such a way, may reach a high velocity, exceeding considerably the speed of galaxies in cluster. If the shell meets another cluster, or another shell moving towards, the collision of such flows may induce a particle acceleration. Due to high speed, large sizes, and low density such collisions may create cosmic rays of the highest possible energy (EHECR). We may expect the largest effect when two clusters move to each other. The influence of DE is decreasing with with a red shift, therefore the acceleration of EHECR in this model should take place in the periphery, or between, the closest rich galaxy clusters. The example of collision of two clusters of galaxies was given in observations of Clowe et al. (2006). The structure of two colliding stellar winds was calculated by Eichler and Usov (1993), and it has some similarities with the structure of the colliding clusters.

After quitting the cluster the gas is moving with acceleration, acting as a snowplough for the intergalactic gas. The shell of matter, forming in such a way, may reach a high velocity, exceeding considerably the speed of galaxies in cluster. If the shell meets another cluster, or another shell moving towards, the collision of such flows may induce a particle acceleration. Due to high speed,

large sizes, and low density such collisions may create cosmic rays of the highest possible energy (EHECR). We may expect the largest effect when two clusters move to each other. The influence of DE is decreasing with with a red shift, therefore the acceleration of EHECR in this model should take place in the periphery, or between, the closest rich galaxy clusters. Note, that similar mechanism of particle acceleration is expected in collision of two stellar winds (Eichler and Usov, 1993), but in much lower energy region.

7. Conclusions

The density of DE, measured from SN Ia distributions, and spectra of fluctuations CMB perturbations, imply the necessity to take it into account in calculations of the structure of galaxy clusters.

The existing observational indefiniteness in the parameters of Local cluster, as well as of Virgo and Coma clusters, indicate to the dynamic importance of DE at outer edges of the galaxy clusters.

Hot gas in GC is accelerated in presence of DE, and EHECR may be accelerated in rapid colliding winds from clusters, moving to each other

Acknowledgments The author is grateful to his coauthors A.D. Chernin and M. Merafina for numerous discussion and help in the work, and to Franco Giovannelli for support and hospitality. This work was partly supported by RFBR grants 14-02-00728, 14-29-06045; the RAN Presidium Program P21/3, and Russian Federation President Grant for Support of Leading Scientific Schools NSh-261.2014.2.

8. Acknowledgments

The work of SGM and GSBK was supported partially by RFBR grants 14-02-00728 and 14-29-06045, and by President RF grant NSh-261.2014.2.

References

- [1] G.S. Bisnovaty-Kogan, *Relativistic Astrophysics and Physical Cosmology* [in Russian], URSS Moscow 2011.
- [2] G.S. Bisnovaty-Kogan & A.D. Chernin, *Dark energy and key physical parameters of clusters of galaxies*, *ApSS* **338** (2012) 337.
- [3] G.S. Bisnovaty-Kogan & M. Merafina, *Galactic cluster winds in presence of a dark energy*, *MNRAS* **434** (2013) 3628.
- [4] A.D. Chernin, *Cosmic vacuum*, *Physics-Uspokhi* **44** (2001) 1099.
- [5] A.D. Chernin, *Dark energy and universal antigravitation*, *Physics-Uspokhi* **51** (2008) 253.
- [6] A.D. Chernin, G.S. Bisnovaty-Kogan, P. Teerikorpi, et al., *Dark energy and the structure of the Coma cluster of galaxies*, *A&A* **553** (2013) 101.
- [7] D. Clowe, M. Bradač, A.H. Gonzalez, et al., *A Direct Empirical Proof of the Existence of Dark Matter*, *ApJ* **648** (2006) L109.

- [8] D. Eichler & V.V. Usov, *Particle acceleration and nonthermal radio emission in binaries of early-type stars*, *ApJ* **402** (1993) 271.
- [9] E.B. Gliner, *Algebraic Properties of the Energy-momentum Tensor and Vacuum-like States of Matter*, *Soviet Physics JETP* **22** (1966) 378.
- [10] I.D. Karachentsev, A. Dolphin, R.B. Tully, et al., *Advanced Camera for Surveys Imaging of 25 Galaxies in Nearby Groups and in the Field*, *AJ* **131** (2006) 1361.
- [11] D. Larson, J. Dunkley, G. Hinshaw, et al., *Seven-year Wilkinson Microwave Anisotropy Probe (WMAP) Observations: Power Spectra and WMAP-derived Parameters*, *Astrophys.J.Suppl.* **192** (2011) 16.
- [12] M. Merafiva M., G.S. Bisnovatyι-Kogan, & S.O. Tarasov, *A brief analysis of self-gravitating polytropic models with a non-zero cosmological constant*, *Astron. Ap.* **541** (2012) 84.
- [13] E.N. Parker, *Interplanetary dynamical processes*, New York, Interscience Publishers 1963.
- [14] S. Perlmutter, S. Gabi, G. Goldhaber, et al., *Measurements of the Cosmological Parameters Ω and Λ from the First Seven Supernovae at $z \geq 0.35$* , *Astrophys. J.* **483** (1997) 565.
- [15] S. Perlmutter, G. Aldering, G. Goldhaber, et al., *Measurements of Ω and Λ from 42 High-Redshift Supernovae*, *ApJ* **517** (1999) 565.
- [16] Planck Collaboration. *Planck 2013 results. XVI. Cosmological parameters*, *Astronomy & Astrophysics* **571** (2014) A16 [astro-ph 1303.5076].
- [17] W.H. Press, S.A. Teukolsky, W.T. Vetterling, B.P. Flannery, *Numerical Recipes in Fortran 77: The Art of Scientific Computing*, Cambridge Univ. Press 1992.
- [18] A.G. Riess, A.V. Filippenko, P. Challis, et al., *Observational Evidence from Supernovae for an Accelerating Universe and a Cosmological Constant*, *AJ* **116** (1998) 1009.
- [19] A.D. Sakharov, *The initial stage of an expanding universe and the appearance of a nonuniform distribution of matter*, *ZhTEP* **49** (1965) 345 [Soviet Physics JETP **22** (1966) 241].
- [20] B.P. Schmidt, N.B. Suntzeff, M.N. Phillips, et al. *The High-Z Supernova Search: Measuring Cosmic Deceleration and Global Curvature of the Universe Using Type IA Supernovae*, *Astrophys. J.* **507** (1998) 46.
- [21] D.N. Spergel, L. Verde, H.V. Peiris, et al. *First-Year Wilkinson Microwave Anisotropy Probe (WMAP) Observations: Determination of Cosmological Parameters*, *Astrophys. J. Suppl.* **148** (2003) 175.
- [22] D.N. Spergel, R. Flauger, & R. Hložek, *Planck Data Reconsidered* *Phys.Rev.* **D91** (2015) 023518 [arXiv:1312.3313].
- [23] K.P. Stanyukovich, *Unsteady Motions of Continua* [in Russian], Gostekhizdat 1955.
- [24] M. Tegmark, M.A. Strauss, M.R. Blanton, et al. *Cosmological parameters from SDSS and WMAP*, *Phys. Rev.* **D69** (2004) 103501.
- [25] M. Watanabe, K. Yamashita, A. Furuzawa, et al. *Temperature Map of the Coma Cluster of Galaxies*, *Astrophys. J.* **527** (1999) 80.

DISCUSSION

D. BISIKALO: 1. Why do you consider the solution without self-gravity term?

2. Does the radiative cooling important for colliding wind shocks (for accelerating of cosmic rays)?

G. BISNOVATYI-KOGASN: 1. The wind is very rarefied, and its self-gravity may be neglected.

2. Here only wind acceleration is considered, where cooling is very small because of alow density.

The consideration of the process in the shock, at wind collision, is another problem, where CR acceleration together with different cooling mechanisms should be analyzed.